Chapter 6

CHAPTER - 6

A CLASS OF SLIPLINE FIELD SOLUTIONS WITH MIXED STRESS AND VELOCITY BOUNDARY CONDITION FOR METAL-MACHINING WITH SLIPPING AND STICKING ZONE AT THE CHIP/TOOL INTERFACE WITH ELASTIC CONTACT

6.1 Introduction

An elastic contact length beyond the zone of plastic contact was considered in the solutions presented in chapter 4 and 5. This was necessary to make the above slipline field solutions statically admissible. Further, solutions obtained with the assumption of an elastic contact region yield results more consistent with experimental observations. It is now known that the effect of elastic spring back of the chip onto the tool are more important than work hardening in causing discrepancies between theory and experiment[45]. By the time the material has crossed the equivalent shear plane, most of the hardening has occurred and this is the reason why non-hardening theory gives such good qualitative predictions of chip-curl, chip-thickness and contact length. It is also reported recently in one FEM modeling of orthogonal machining using DEFORM FEM code[85] that the cutting force and strain remain almost unaffected with change in cutting speed.

The shortcomings of the analysis based on the assumption of a rigid-perfectly plastic material has been discussed in detail by Childs[60] in connection with the slipline field model proposed by Dewhurst[55]. He has clearly stated that only with respect to the relation between (ϕ - α) and λ do the experimental results lie mainly within the rigid-perfectly plastic solution ranges where, ϕ is the shear plane angle, α is the rake angle and λ is the friction angle. When estimation of parameters such as friction force, cutting force or contact length etc. are considered, the rigid-perfectly plastic theory is inadequate.

In the present chapter, the modified Dewhurst fields based on the rigid-perfectly plastic material model (chapter - III) have been re-analysed with the incorporation of elastic contact forces beyond the zone of plastic contact by regarding them as externally applied forces on the chip. Solutions are obtained both for parabolic and exponential normal stress distributions in the elastic contact region. A constant ratio of elastic to plastic contact length is assumed. Analysis is carried out when both sticking and slipping zones are present in the plastic contact region (high μ) or when the plastic contact region is governed by slipping friction only (low μ). The variation of normal and shear stresses at the chip-tool interface with variation in coefficient of friction as well as rake angles is predicted. The normalised cutting forces, cutting ratio, radius of chip curl, natural contact length, sticking length and sticking ratio are evaluated for different rake angles and for different coefficients of friction. Experimental results available in literature are compared with theory and are found to be satisfactory.

6.2 Methodology

The two slipline fields under consideration are shown in Fig 6.1 and 6.2 along with their associated hodographs. Solution I (Fig 6.1) applies when the friction stress τ on the chip/tool boundary no where equals the yield stress k in shear (full slipping). Solution II (Fig 6.2) applies when both sticking and slipping zones exist at the chip-tool interface (refer to section 3.2). To introduce elastic effects into the present analysis , an elastic contact length beyond the length of plastic contact was assumed as discussed in chapter 4 & 5. In the plastic zone, the normal and shear stresses were assumed to be governed by the proposed slipline fields. In the length of elastic contact, the normal pressure was assumed to be distributed either exponentially or parabolically. For any given pressure distribution in the elastic contact length the forces H_E, V_E and elastic moment M_E are readily calculated (chapter - 4). The forces H_P, V_P and the moment M_P for the slipline curves defining the chip boundary can be evaluated with the help of the matrix operational procedure as explained in detail in chapter - III. For equilibrium of the chip, the forces and moment in the elastic contact region together with those at the chip boundary must simultaneously be equal to zero. Mathematically, the above condition may be stated as,

$$F_1 = H_P - H_E = 0 \qquad 6.1\,(a)$$

$$F_2 = V_P - V_E = 0 \qquad 6.1\,(b)$$

$$F_3 = M_P - M_E + H_E L_H + V_E L_V = 0 \qquad 6.1(c)$$

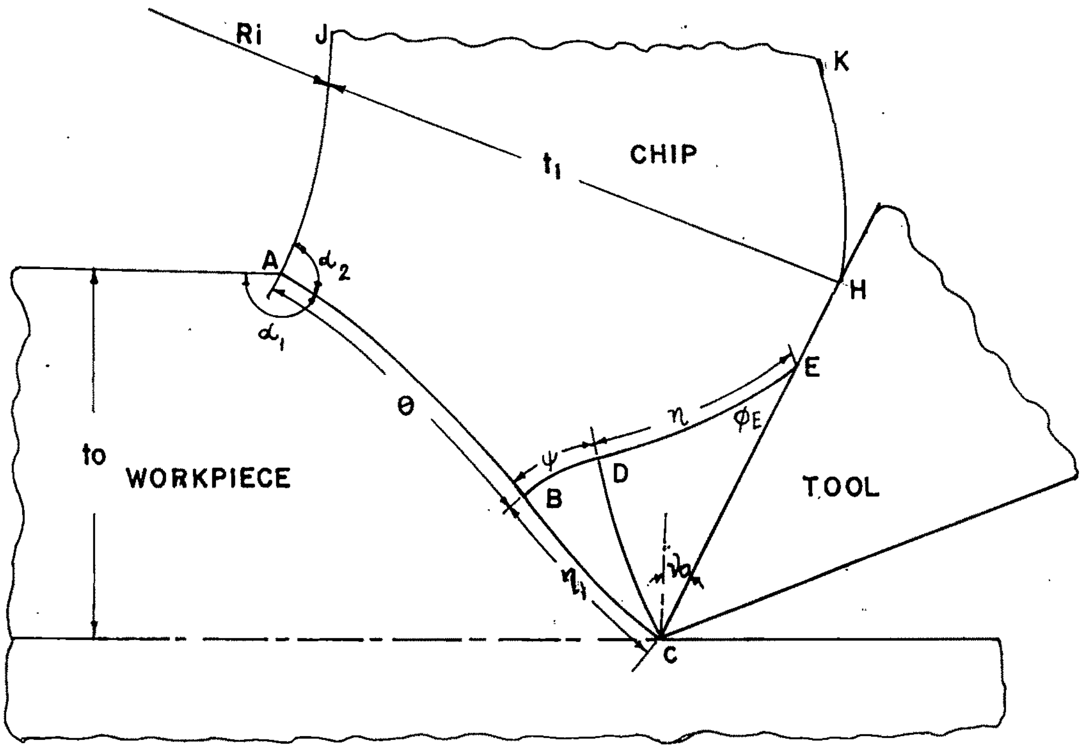

FIG. 6.1(a) SLIPLINE FIELD

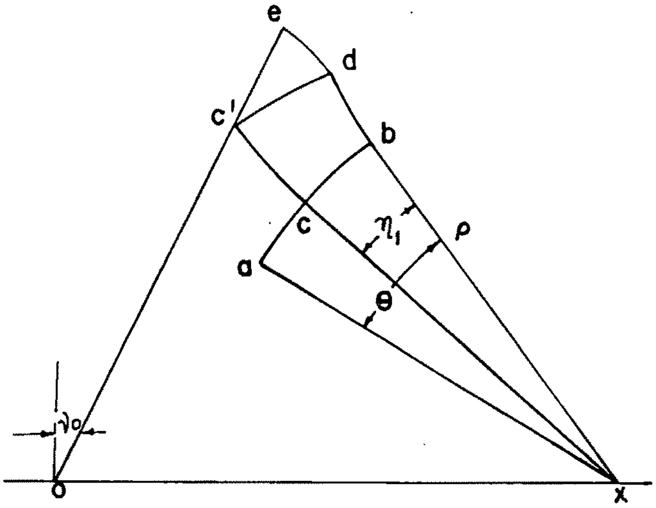

FIG. 6.1 (b) HODOGRAPH

SOLUTION-I

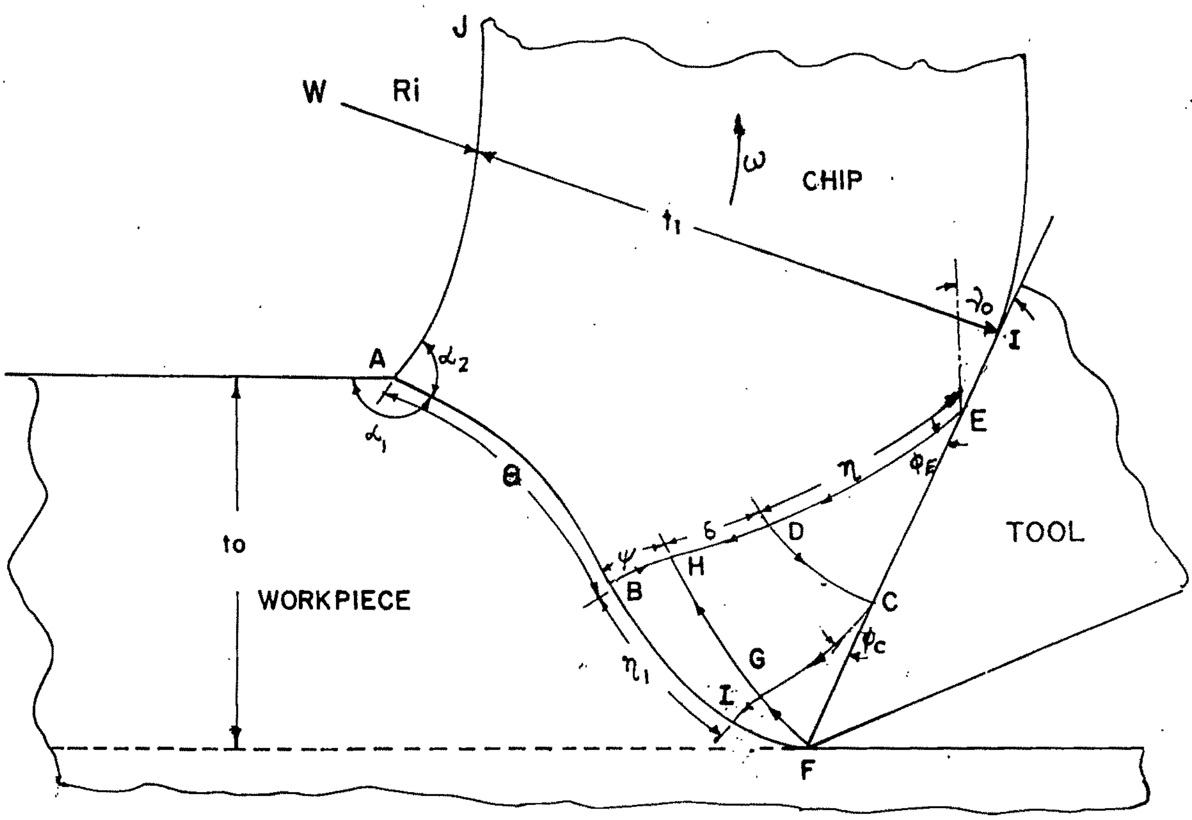

FIG. 6.2(a) SLIPLINE FIELD

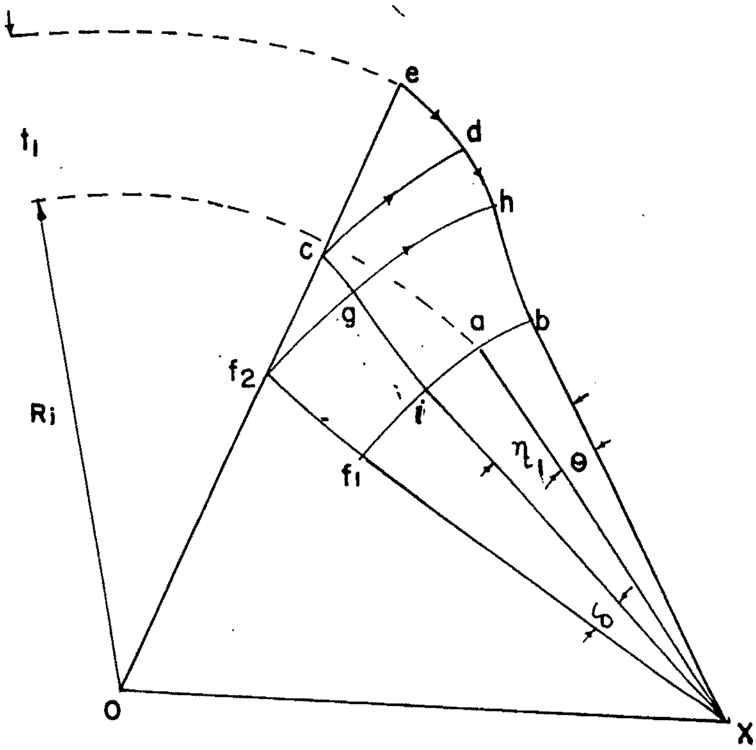

FIG. 6.2(b) HODOGRAPH

SOLUTION-II

A FORTRAN programme developed for analysing the above fields calculated the forces H_P, V_P and moment M_P in the chip-boundary using the subroutines in [49], [55] and [65]. For any given value η or δ and prescribed pressure distribution in the elastic contact zone (parabolic or exponential), the programme then solved the above set of non-linear algebraic equations with the help of an algorithm developed by Powell[51]. Equilibrium was assumed to be achieved when the values of θ, P_E and ψ computed in the above manner satisfied the inequality:

$$(F_1 / kt_0)^2 + (F_2 / k\, t_0)^2 + (F_3 / k\, t_0\, t_0)^2 \leq 10^{-10} \qquad (6.2)$$

The programme then used the values of the optimised field variables to compute the machining parameters such as the cutting ratio, radius of chip curl , tangential cutting force, thrust force, total contact length, sticking contact length and sticking ratio. It also contained checks to determine whether rigid vertices at A were overstressed. In all calculations, the scale factor ρ/ω was set to equal to 1 and the ratio of the elastic to the plastic contact length was taken equal to1.0. The programme also incorporated the flatness, mass flux and traction checks as explained in section 3.3.

6.3 Results and discussion

The permissible limits of the solution range with the introduction of an elastic contact length is illustrated in Fig.6.3 for values of friction coefficient μ equal to 0.4 and 0.6. Comparing these results with those obtained from the rigid-perfectly plastic analysis

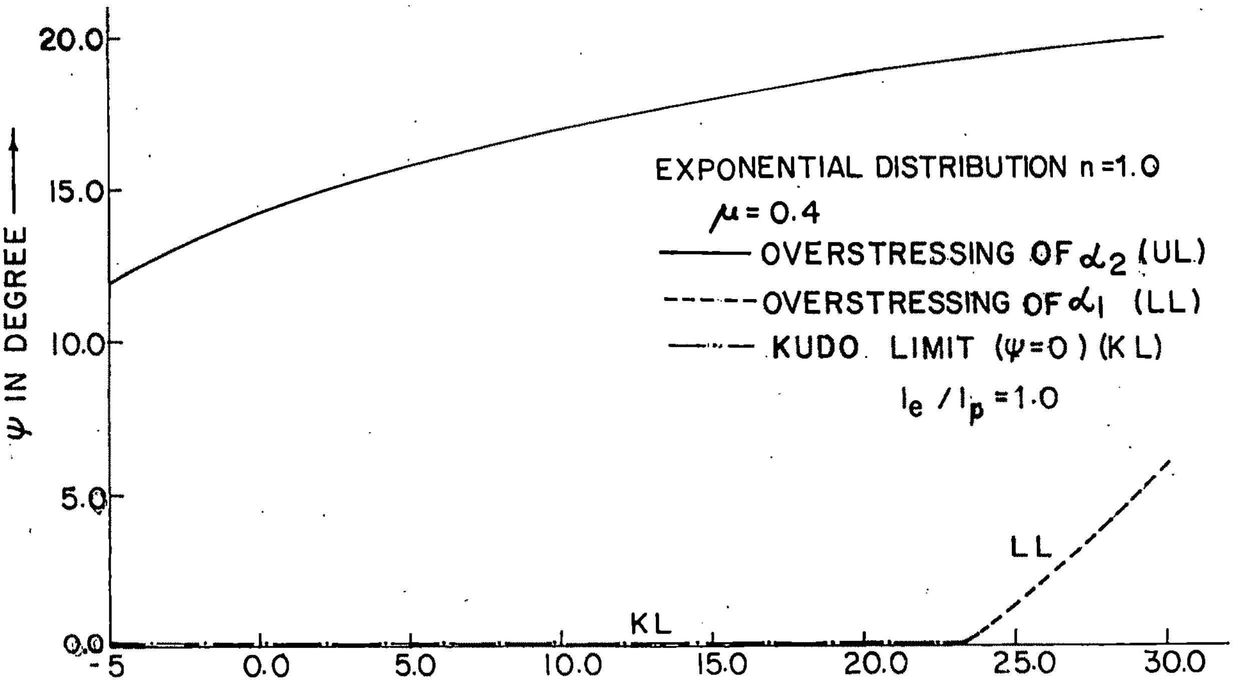

FIG.6.3(a) RANGE OF VALIDITY OF SOLUTION -I (FIG. 6.1)

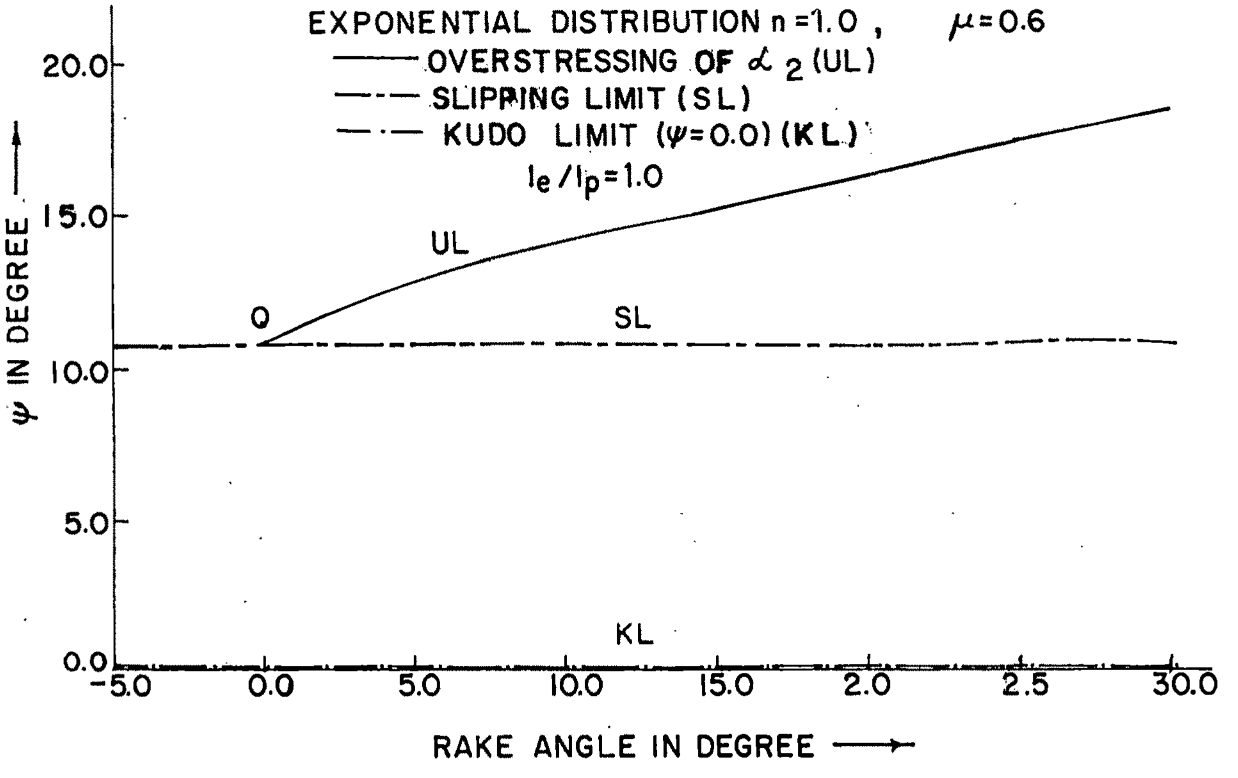

FIG.6.3(b) RANGE OF VALIDITY OF SOLUTION-II (FIG.6.2)

(Fig.3.3 chapter -III) indicates that the incorporation of the elastic contact zone only marginally affects the upper limit of the solution range (curve UL) defined by the overstressing of the vertex angle α_2 at A (Fig.6.1 and Fig. 6.2). Curve LL (overstressing of vertex angle α_1), however, now shifts to the left, meeting the abscissa at $\gamma = 23.5^0$ for $\mu = 0.4$. This was not so in the case of rigid-plastic analysis where α_1 was never overstressed for $\mu \geq 0.4$ for rake angle values between -5 and 30 degrees. Further, the lower limit of the solution range in the present case for $\psi = 0$ is provided by Kudo's slipline field (Fig.5.1) and not by Lee and Shaffer solution which was the case for rigid-plastic analysis (Fig. 3.3).

The variation of machining parameters with rake angles as obtained with the assumption of an elastic contact zone (ratio of elastic to plastic contact length equal to 1.0) are shown in Fig 6.4 -6.7 for μ values equal to 0.4 , 0.6 and 0.8. For each value of the rake angle, the range of possible solutions lie within the limits as discussed with reference to Fig. 6.3. For μ equal to 0.8, only the upper limit of machining parameters (corresponding to overstressing of α_2 at rigid vertex A) are presented. It may be seen with reference to Fig.6.8 that contact length and radius of chip curl are significantly affected in the presence of an elastic contact zone. This is in agreement with the observations made by Childs[60]. Comparison of the present theoretically computed values shows excellent agreement with the experimental results of Eggleston et al.[23] and Ponkshe[35](Fig. 6.4, 6.5 and 6.6). It may also be seen with reference to Fig. 6.9 that when the elastic contact length is assumed equal to the plastic contact length, the elastic contact forces contribute to about 30 to 35% of the total cutting force for $\mu = 0.8$ and to

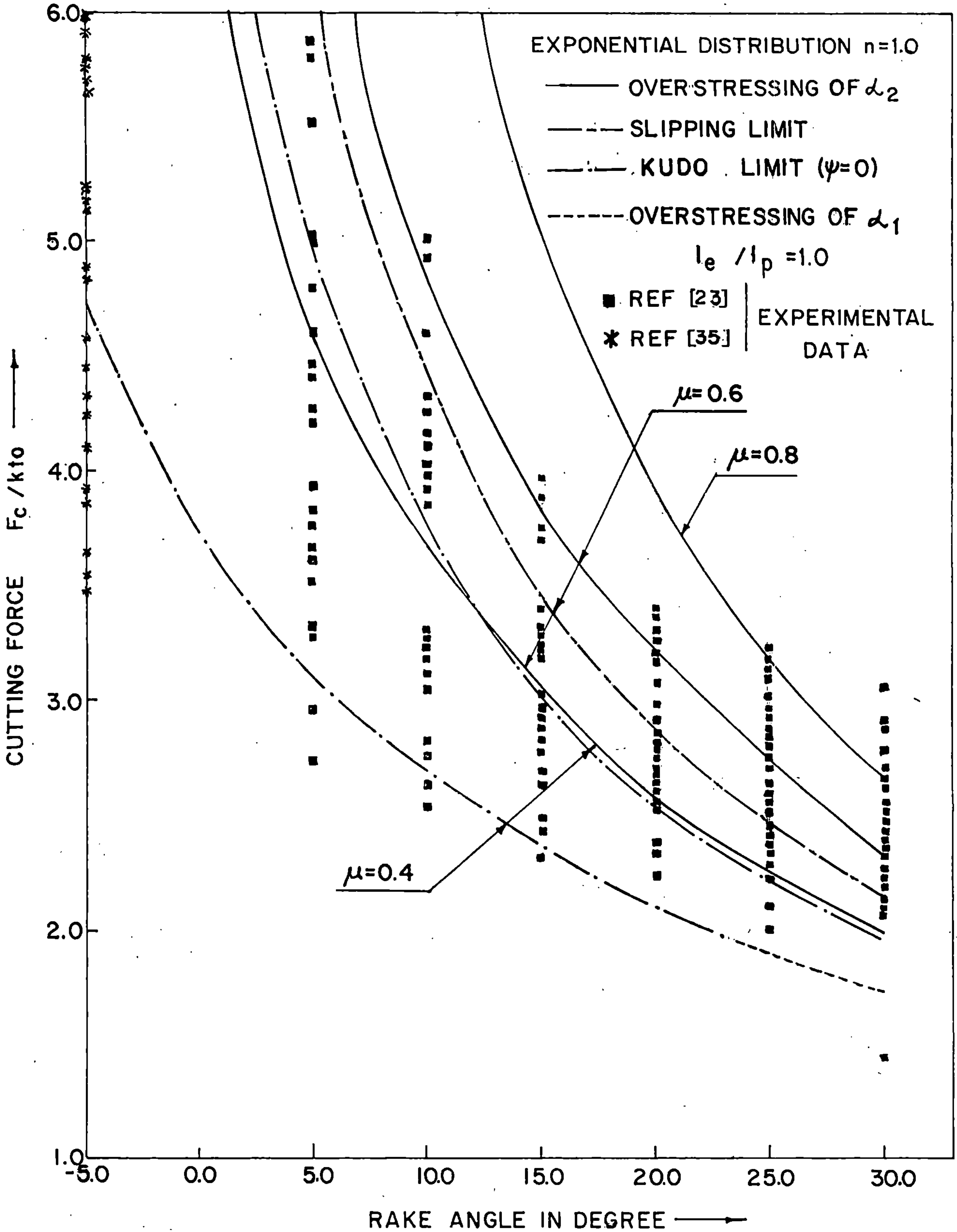

FIG.6.4 VARIATION OF NON-DIEMENSIONALIZED F_c WITH RAKE ANGLE (γ_o) AND FRICTION COEFFICIENT (μ).

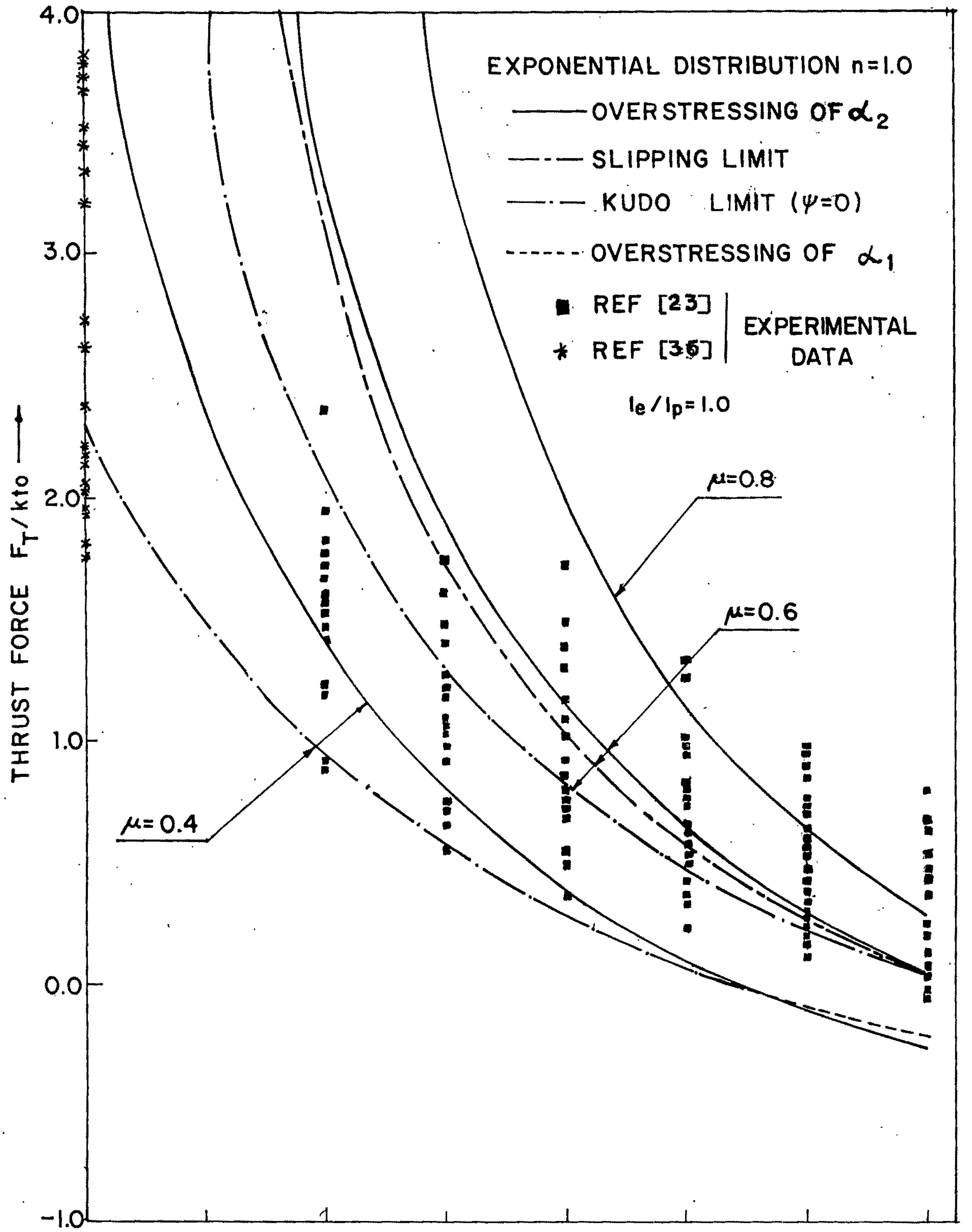

FIG.6.5 VARIATION OF NON-DIMENSIONALIZED F_T WITH RAKE ANGLE(γ_0) AND FRICTION COEFFICIENT(μ).

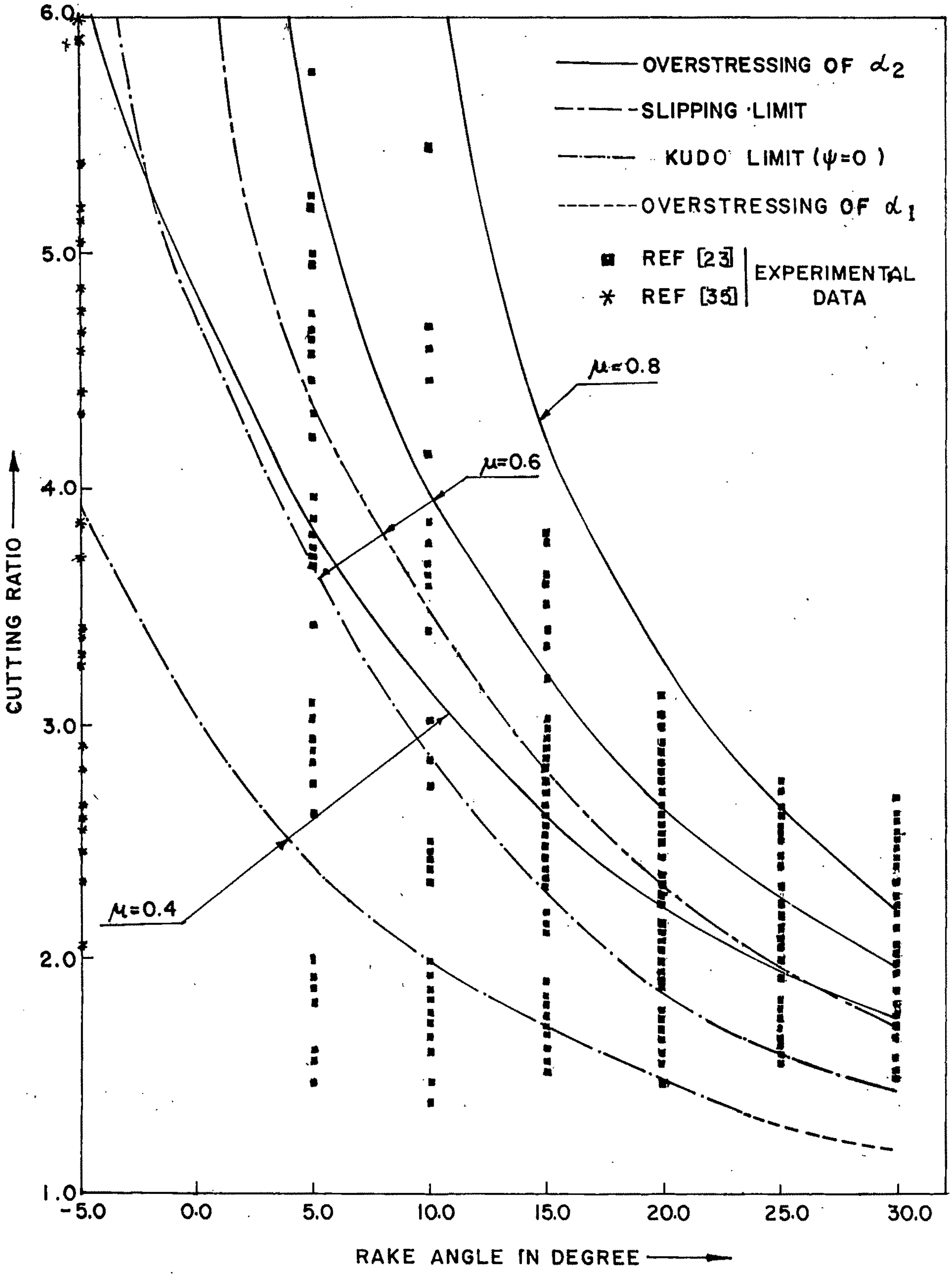

FIG. 6.6 VARIATION OF THE CUTTING RATIO WITH RAKE ANGLE AND FRICTION COEFFICIENT.

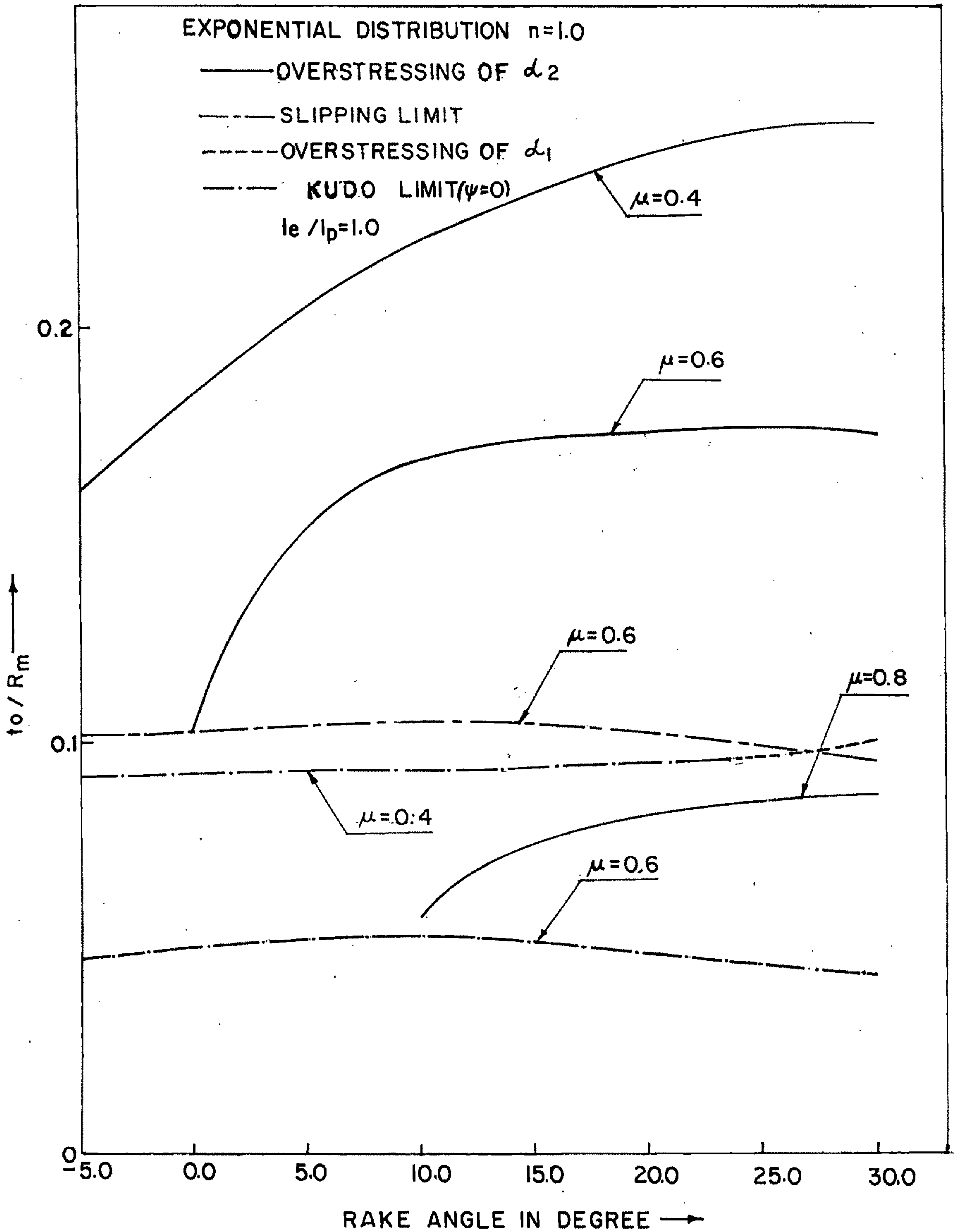

FIG. 6.7 VARIATION OF CURVATURE OF THE MACHINED CHIP WITH RAKE ANGLE AND FRICTION COEFFICIENT

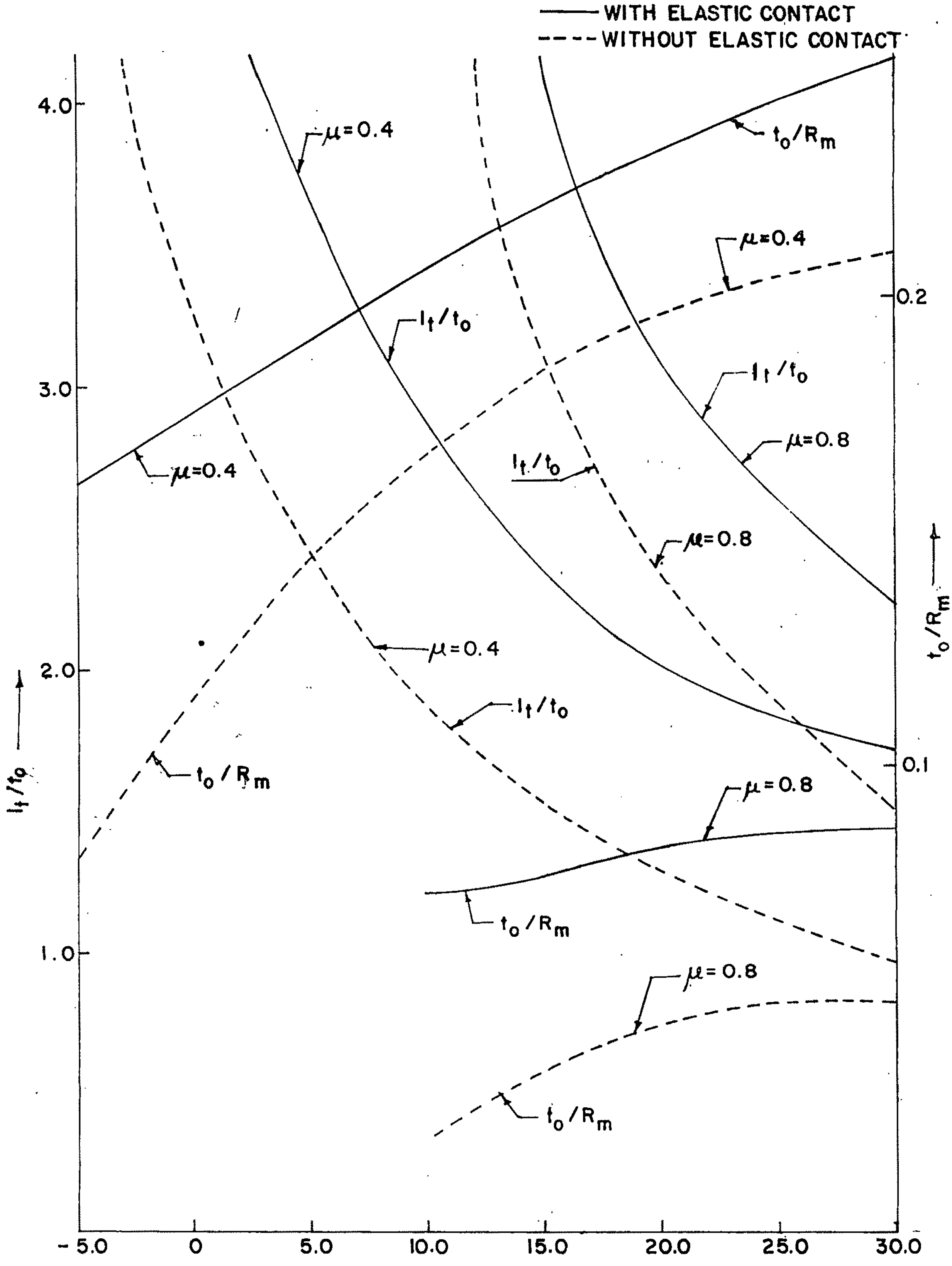

FIG.6.8 COMPARISON OF MACHINING PARAMETERS BETWEEN SOLUTIONS WITH AND WITHOUT ELASTIC CONTACT.

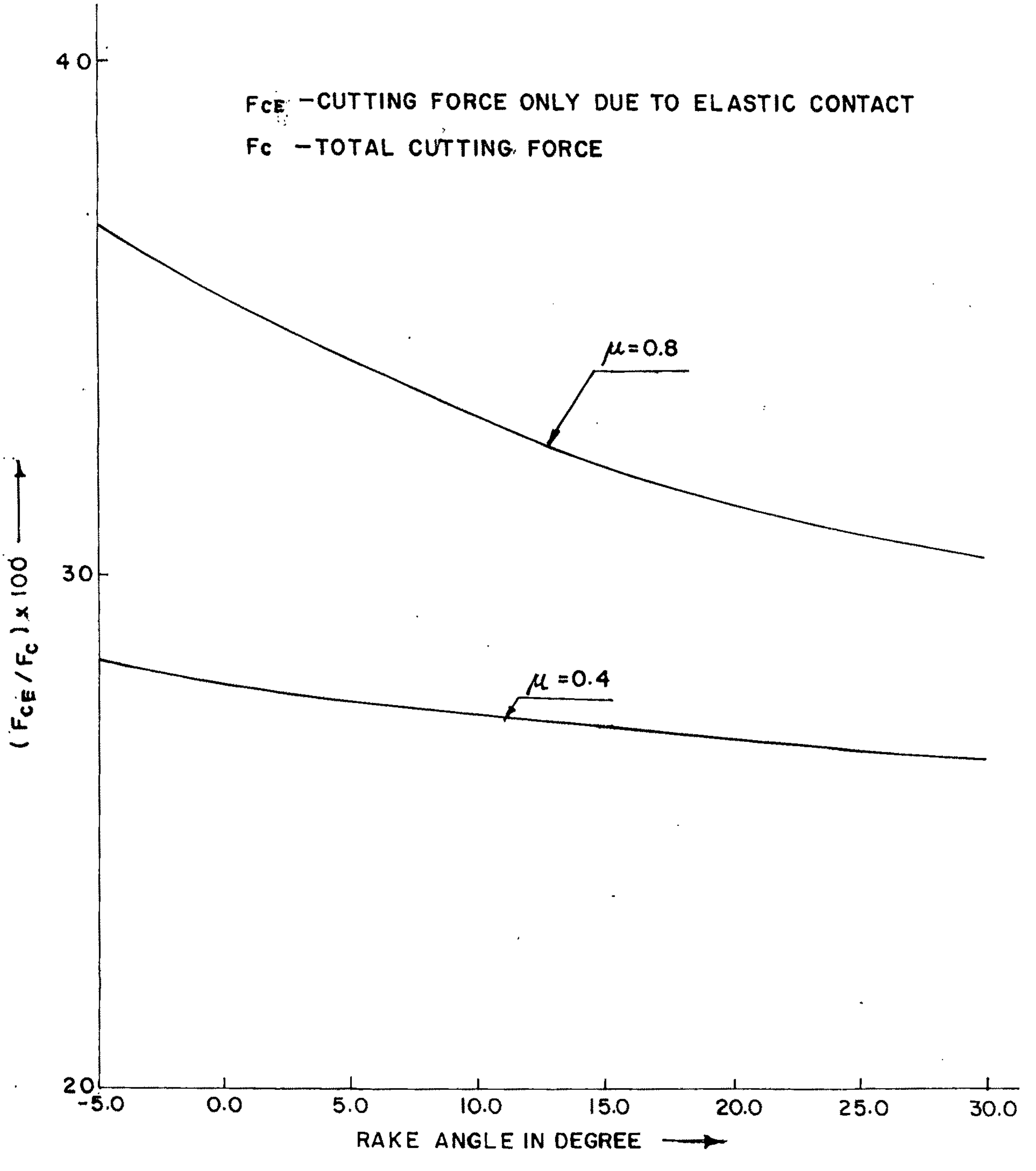

FIG. 6.9 VARIATION OF F_{CE}/F_c WITH RAKE ANGLE

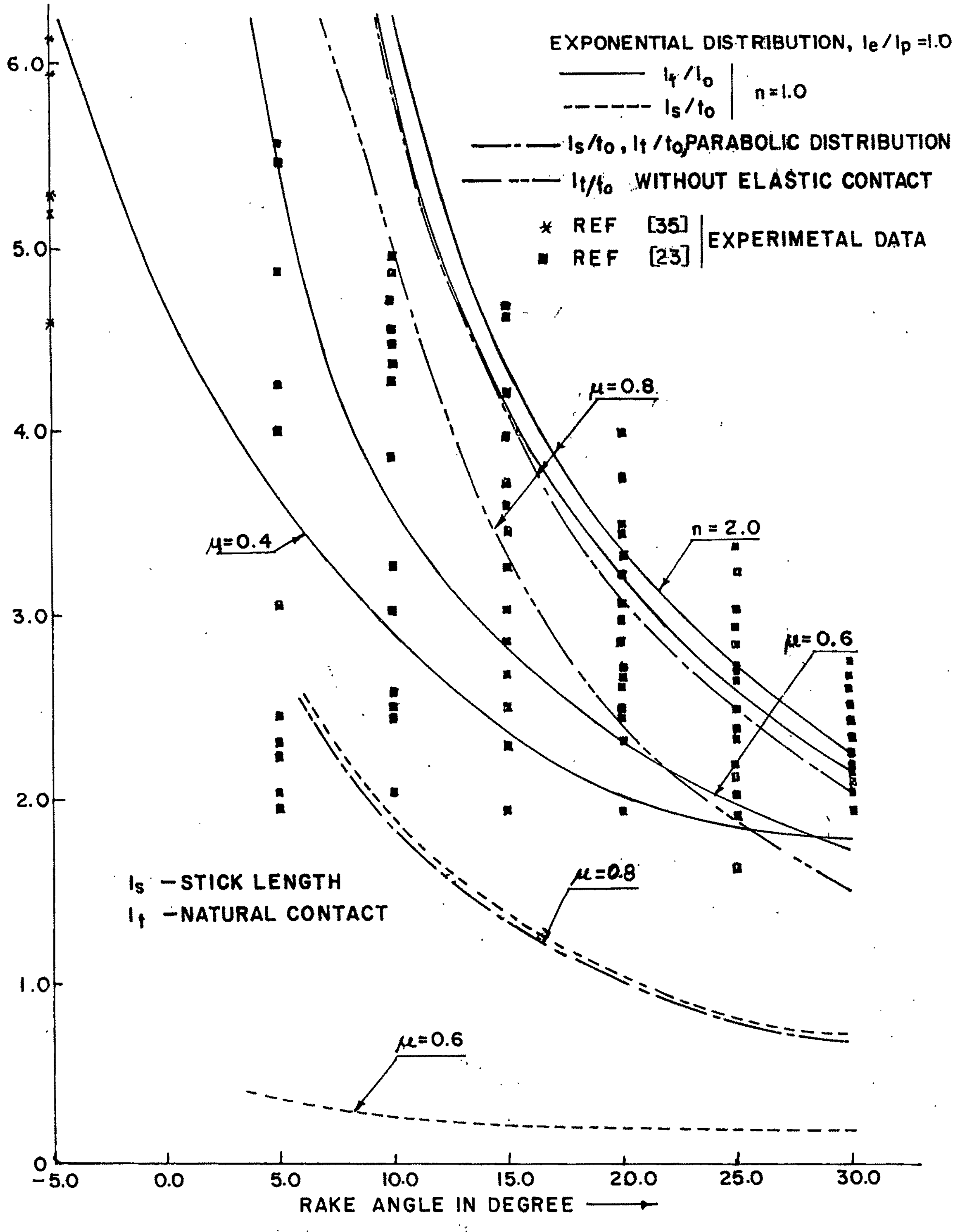

FIG.6.10 VARIATION OF CONTACT LENGTH WITH RAKE ANGLE

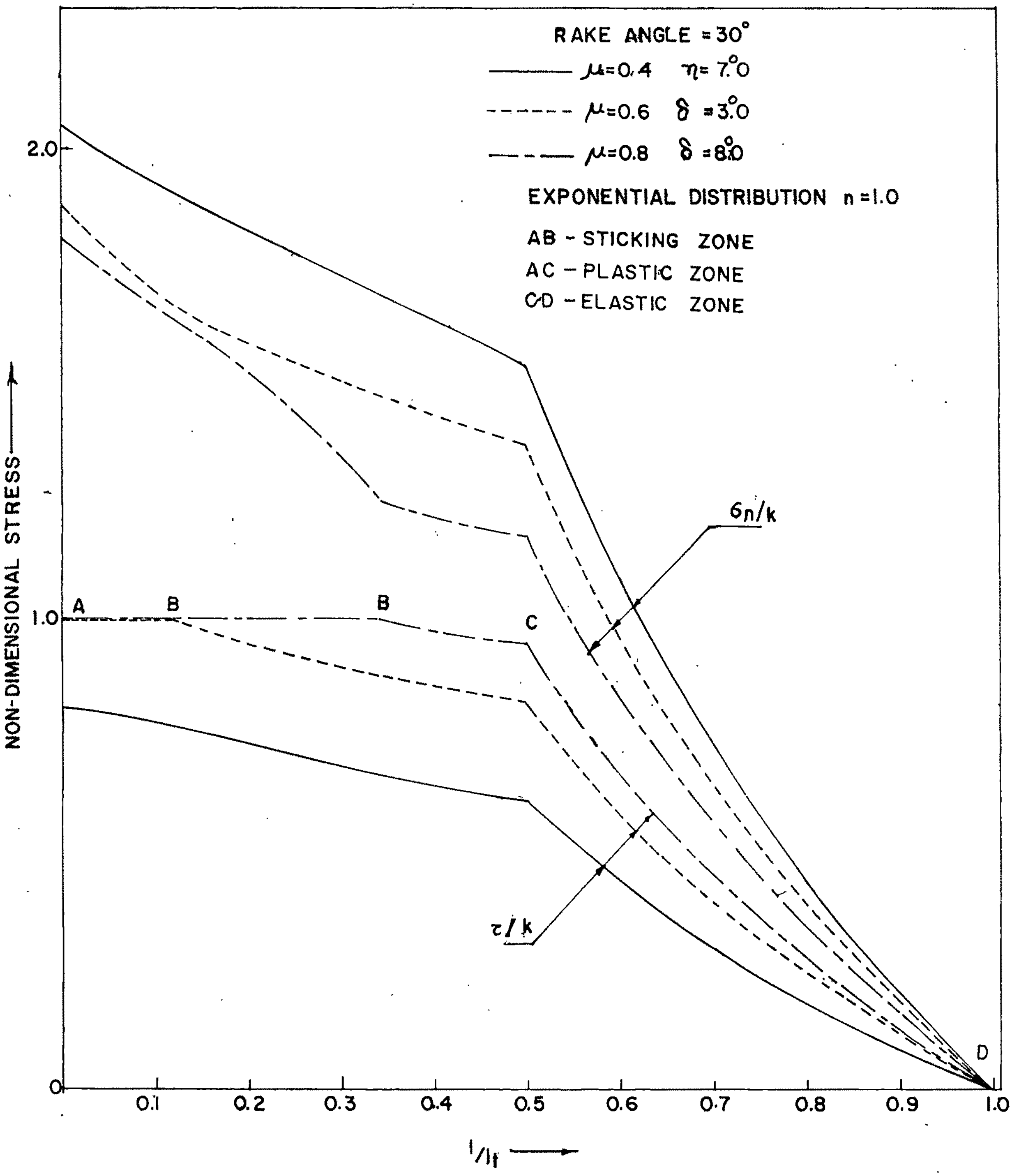

FIG.6.11 VARIATION OF INTERFACE CONTACT STRESS (SOLUTION-I AND II)

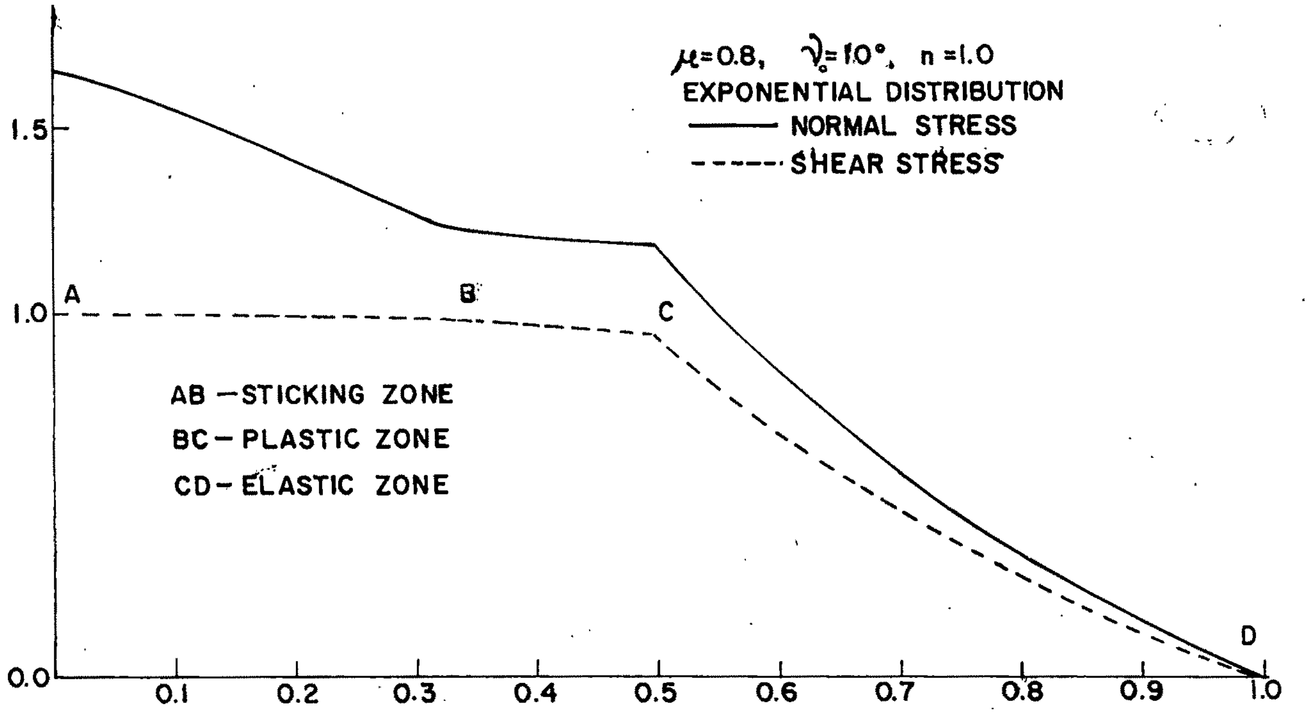

FIG. 6.12(a) VARIATION OF INTERFACE CONTACT STRESS(SOLUTION-II)

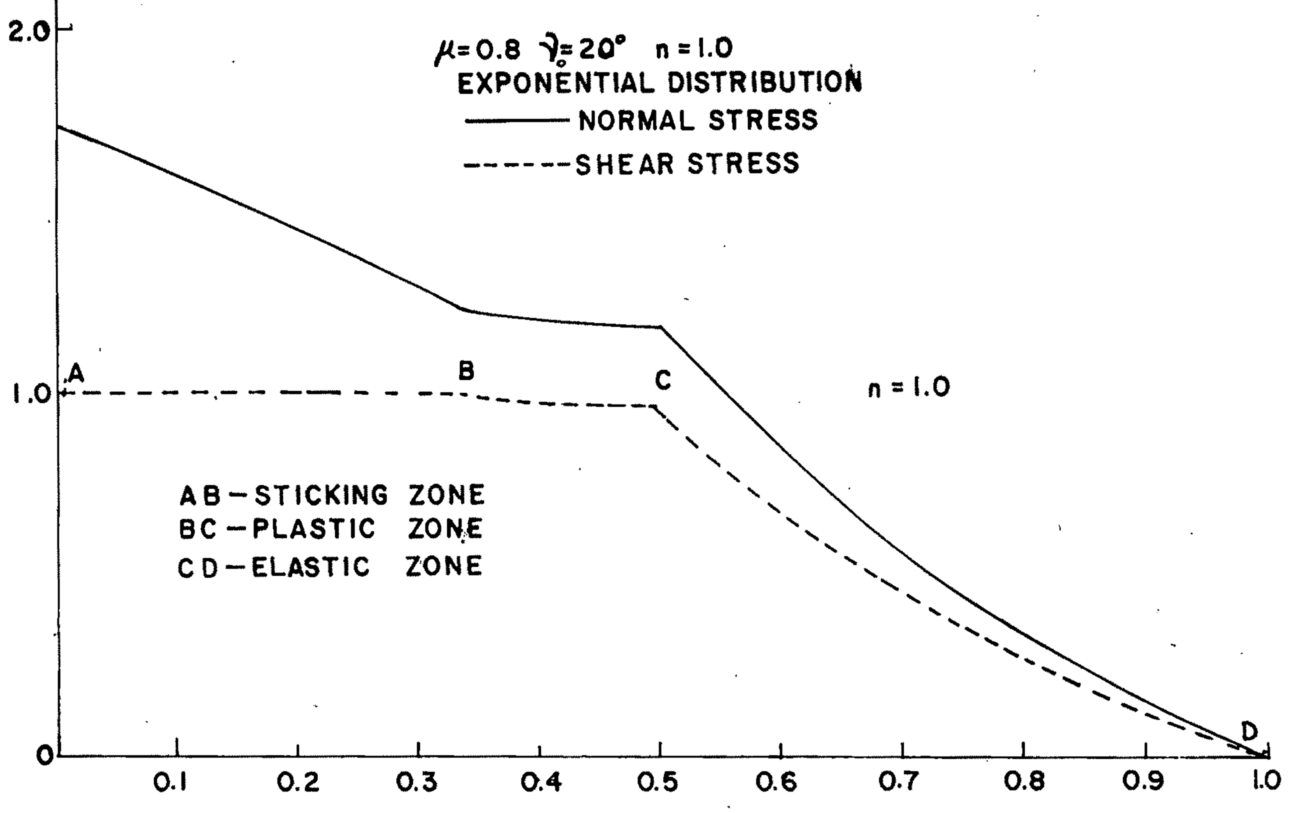

FIG. 6.12 (b) VARIATION OF INTERFACE CONTACT STRESS (SOLUTION-II)

about 26% to 27% when μ = 0.4. This is in agreement with the observations made by Childs[45] who suggested that forces acting in the region of elastic contact can account for upto 40% of the total force on the tool. Estimation of natural contact length based on the assumption of an elastic contact region also shows better agreement with the experimental observations (Fig.6.10) compared to those obtained from rigid-perfectly plastic analysis.

Typical plot of stress distributions with elastic and plastic contact at chip/tool interface is shown in Fig.6.11 and Fig 6.12. The stress distribution shows excellent qualitative agreement with those obtained from experiments[74].

6.4 Conclusion

1. Solutions obtained with the introduction of an elastic contact zone are valid for the case of chip-curling only. The natural contact length and chip curl radius are significantly affected, when an elastic contact zone is incorporated in the slipline field analysis.
2. The forces acting in the elastic zone when the length of elastic contact is equal to that of plastic contact may be of the order of 30 to 35% of total cutting force.
3. The stress distribution shows qualitative agreement with those obtained from experiments.